

# XMM-Newton CCF Release Note

XMM-CCF-REL-263

## 2-D PSF parametrisation

A.M. Read, R. Saxton, M. Guainazzi, S. Rosen, M. Stuhlinger

May 7, 2010

### 1 CCF components

| Name of CCF        | VALDATE    | List of Blocks changed | Change in CAL HB |
|--------------------|------------|------------------------|------------------|
| XRT1_XPSF_0011.CCF | 2000-01-01 | ELLBETA_PARAMS         | YES              |
| XRT2_XPSF_0011.CCF | 2000-01-01 | ELLBETA_PARAMS         | YES              |
| XRT3_XPSF_0011.CCF | 2000-01-01 | ELLBETA_PARAMS         | YES              |

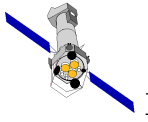
### 2 Change

We are introducing a full 2-D parametrisation of the EPIC PSF as a function of instrument, energy and off-axis angle, covering the whole field-of-view. It models the PSF spokes and the large-scale azimuthal variations, and includes an additional Gaussian core, which accounts for (at most) 2% of the enclosed energy flux in the MOS cameras. This version is not fully scientifically validated, and some areas of the parameter space have still to be explored and/or refined.

The primary reasons for making the 2-D PSF parametrisation available within the CCF at this time are to facilitate the ongoing testing/refinements and to simplify the development of the SAS software that uses it. For this reason, it is not employed as the default PSF by any of the SAS 10 software. We stress very strongly that use of the 2-D PSF by users is generally deprecated but that if it is used, resulting analysis should be treated with extreme caution.

#### 2.1 A full 2-D PSF parametrisation

Three physical ingredients enter into the 2-dimensional (2-D) PSF parametrisation introduced with this CCF:



- a (currently) position-angle independent parametrisation of the elliptical PSF envelope as a function of camera, energy, and off-axis angle. An additional Gaussian “core” is added to the PSF envelope of the MOS cameras for low and medium energies ( $E \leq 6$  keV) only. The relevant parameters are included in the `ELLBETA_PARAMS` extension.
- an azimuthal filter of the elliptical envelope, which describes the effect of the star-like pattern (“spokes”) created by the spider supporting the 58 co-axial mirrors of each telescope<sup>1</sup>. The parameters of this filtering (Sect. 2.1.2) are currently hard-coded into the CAL software.
- a further azimuthal dependency of the overall PSF envelope, which is responsible for the apparently triangular shape of the MOS2 PSF. At a lower lever, a similar effect may be present in the PSF of all the cameras. Currently, this correction is applied to the PSFs of MOS1 and MOS2 only. The parameters of this correction (see Sect. 2.1.3) are currently hard-coded into the CAL package.

### 2.1.1 Elliptical envelope

The shape of the overall PSF envelope has for the first time been determined by stacking a large number ( $>250$  observations) of good quality, long-exposure, non piled-up, bright EPIC point sources from the full field-of-view of each EPIC detector. Flare-cleaned and background-subtracted images of individual sources have been brought to a common reference frame in detector coordinates and stacked in 8 energy bins (linear midpoints: 0.55, 1.5, 2.75, 4.25, 6, 8, 10.25, 13.25 keV) and 6 off-axis angle bins (0', 3', 6', 9', 12', 15') for each camera.

These stacked images were fit with a 2-D King profile (a `beta2d` model in CIAO-SHERPA) :

$$B(r) = \frac{A}{[1 + (r/r_0)^2]^\alpha}$$

where:

$$r(x, y, \theta) = \sqrt{[(x \cos \theta + y \sin \theta)^2] + [(y \cos \theta - x \sin \theta)^2]/(1 - \epsilon)^2}$$

$r_0$  (core radius),  $\alpha$ , and  $\epsilon$  (ellipticity) are the model parameters.

To the parametrisation above, a further 2-D Gaussian “core” has been added to model excess emission in the low- and medium-energy ( $E \leq 6$  keV) PSF at the very centre of the MOS cameras (no such core is seen to be necessary for pn). Again, the model implicitly includes an ellipticity term through the definition of the  $r$  variable as above. The 2-D Gaussian function used (*gaus2d* model in CIAO-SHERPA) is :

$$G(r) = A e^{-4 \ln(2) (r/\text{FWHM})^2}$$

where FWHM is the full width at half maximum.

---

<sup>1</sup>An image of the mirror structure is available in the XMM-Newton Gallery:  
<http://xmm.esac.esa.int/external/xmm-science/gallery/public/level3.php?id=65>

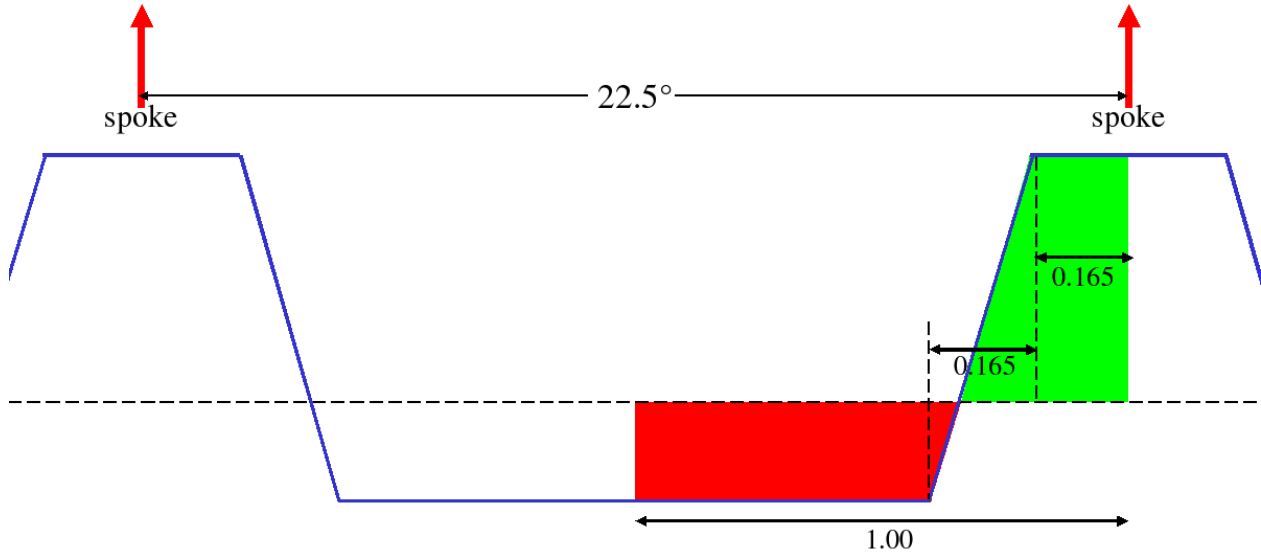


Figure 1: Scheme of the flat-topped triangular function used to parametrise the PSF “spokes”. The *red* and the *green* areas exactly cancel out. “1.00” and “0.165” are in units of half the infra-spoke distance, *i.e.*  $11.25^\circ$ . The figure is not to scale.

### 2.1.2 Spokes

The radial spokes have been modelled with a flat-topped triangular function (Fig. 1). 16 equally-spaced spokes have been included in the model. The distance between two consecutive peaks of the spoke function is therefore  $22.5^\circ$ . The shape of this function has been tuned in such a way that it does not change the integral of the radial profile (*i.e.*, the *red* and the *green* areas in Fig. 1 exactly cancel out). This filtering function is fixed in space with respect to the detector, such that any axis of the DETX/Y (or RAWX/Y) coordinate system lies exactly between two spokes, and is only applied to the elliptical envelope *after* this has been rotated according to the azimuthal position of the source on the detector.

16 secondary spokes, observed in very bright sources, and situated between the main primary spokes, are modelled with the same function, rotated by  $11.25^\circ$  with respect to the main spoke system, and with a relative intensity of 6.5%.

### 2.1.3 Large-scale azimuthal modulation

The apparent triangular shape of the MOS2 PSF is due to a spatial low frequency overall modulation of the PSF shape. A pentagonal modulation is also present at a lower level in the MOS1 and pn PSF.

In the current CCF, this modulation is modelled with a multi-peaked cosine function in the PSFs of the MOS cameras:

$$M(\phi) = A \cos(n\phi - \phi_0)$$

Table 1: Parameters of the large-scale azimuthal multi-peak cosine modulation

| Cameras | $A$ | $n$ | $\phi_0$   |
|---------|-----|-----|------------|
| MOS1    | 13% | 5   | $62^\circ$ |
| MOS2    | 45% | 3   | $50^\circ$ |

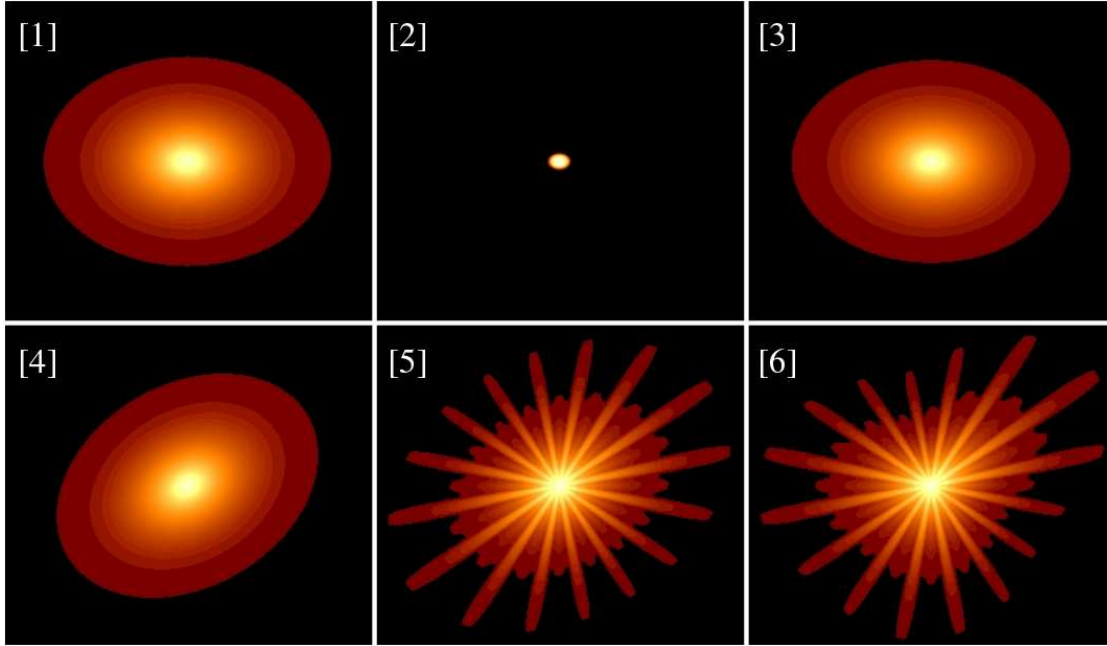
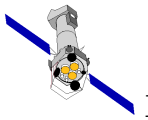


Figure 2: The six steps in the formation of the full 2-D PSF for a source in a given instrument, of a given energy and at a given off-axis and azimuthal angle: [1] The elliptical (**beta2d**) component is constructed, then the Gaussian (**gaus2d**) core [2] is constructed, and these are added [3] in the correct ratio (the CCF parameters in steps 1-3 are all functions of instrument, energy and off-axis angle). Then this is rotated [4] according to the azimuthal position of the source on the detector, and only then are the primary and secondary spoke structures azimuthally filtered in [5], using a flat-topped triangular function. Finally [6] the large-scale azimuthal modulation (a function of EPIC instrument) is filtered in. The example shown is for MOS2.

The parameters of this function are shown in Tab. 1.  $\phi$  runs clockwise from north for a source on the sky, for an observation Position Angle  $PA = 0$ .

#### 2.1.4 Summary

A scheme of the different physical ingredients of the 2-D PSF parametrisation and their effects is shown in Fig. 2. For more details on the 2-D PSF, readers are referred to Read et al. (in preparation).



## 2.2 Description of the CCF parameters

### 2.2.1 Extension ELLBETA\_PARAMS

The extension `ELLBETA_PARAMS` in the PSF CCF files contains the parameters describing the elliptical envelope and the Gaussian core. This extension contains four columns:

- **ENERGY**: the energy (in eV) to which the parameters refer
- **THETA**: the off-axis angle (in radians) to which the parameters refer
- **PHI**: the azimuthal angle (in radians) to which the parameters refer
- **PARAMS**: an array, containing the parameters of the 2-D King (`beta2d`) plus Gaussian (`gaus2d`) function:
  - 1: the `beta2d` core radius ( $r_0$ ), in arcseconds
  - 2: the `beta2d` power-law slope ( $\alpha$ )
  - 3: the ellipticity ( $\epsilon$ ) (of both the `beta2d` and the `gaus2d` components)
  - 4: the `gaus2d` Full Width Half Maximum (FWHM), in arcseconds
  - 5: the normalisation ratio of the `gaus2d` peak to the `beta2d` peak ( $N$ )

## 3 Scientific impact of this update

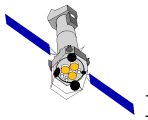
The aims of this update are twofold:

### 3.1 Source searching

A good representation of the 2-D PSF will allow the source-searching software to more accurately calculate source extension and source flux. The better characterisation of the photon distribution will also reduce the number of spurious sources which are seen in the halo of bright sources.

### 3.2 Encircled energy correction

This parametrisation of the PSF uses all of the available high quality, in-orbit data. It should give a more accurate estimation of the flux lost out of the source extraction region, especially at high energies and large off-axis angles where data are sparse.



## 4 Estimated scientific quality

The CCF parameters are still under testing and an estimate of the scientific quality is not yet available.

## 5 Test procedure and results

### 5.1 Spatial comparisons

The source searching procedure currently uses the MEDIUM mode PSF, which is based on images produced by ray-tracing simulations. In Fig. 3 we show a visual comparison of the old and new model PSFs compared with real data. The 0.5-1 keV images of high statistic, non-piled-up on-axis sources, observed with the MOS2 camera, have been rotated to a common reference frame and stacked. The resultant image has been fitted with the MEDIUM and ELLBETA mode PSFs where only the normalisation has been allowed to vary. Residuals are shown in two forms: in units of  $\chi^2 \equiv \sum_{i=1}^N [(D_i - M_i)^2]/M_i$ , where  $D_i$  and  $M_i$  are the value of the data and PSF image in each pixel, and  $N$  is the total number of images; as well as of a merit function  $R \equiv (1/N) \sum_{i=1}^N (D_i - M_i)/|D_i - M_i|$ . The MEDIUM mode PSF leaves strong residuals for several of the spokes and especially for the well known triangular shape of the in-orbit MOS2 source profile. The ELLBETA mode PSF fits much better. Overall a very marked improvement in the 2-D modelling of the MOS2 source profile with the new PSF is apparent. In addition to the spokes and triangles, a ring-like enhancement in the residuals against the MEDIUM PSF is significantly suppressed with the ELLBETA.

A comparison of the radial profiles of a number of sources, at different energies and off-axis angles, with the EXTENDED (circular King function) and ELLBETA mode PSFs, has been made. In general, the PSF fits give similar results but in some off-axis examples the new PSF is giving a better fit (see Fig. 4)

### 5.2 Spectral comparisons

In Fig. 5 we show the residuals of a joint fit of the pn and MOS1/2 cameras for a point source on axis. The upper panel shows the current, EXTENDED, PSF representation while the lower panel shows the fit for the new ELLBETA model. The residuals against a phenomenological model (enhanced from that discussed by Hasinger et al. 2002) are comparable although the fit statistic is a little worse for the ELLBETA model;  $\chi^2/\nu = 746/683$  compared with  $\chi^2/\nu = 693/683$ . A combined instrument fit for a source at 8 arcminutes off axis is shown in Fig. 6. The fit statistic is consistent between the ELLBETA ( $\chi^2/\nu = 594.3/641$ ) and circular ( $\chi^2/\nu = 591.0/641$ ) PSF implementations. In both cases, the elliptical extraction region with ELLBETA was automatically calculated by the SAS task `eregionanalyse` to optimise the source signal-to-noise ratio (Tab. 2). The circular extraction region radius was also calculated to optimise the S/N.

The global effect on source fluxes of changing from the MEDIUM to the ELLBETA PSF is

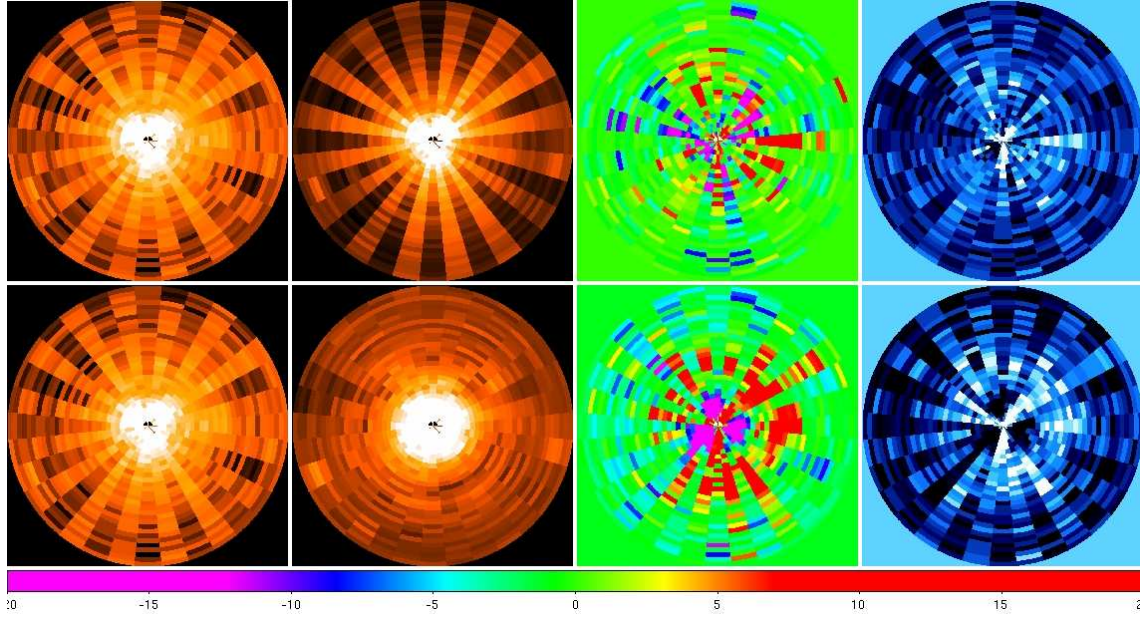


Figure 3: An assessment of the goodness-of-fit of the MEDIUM and ELLBETA mode PSF images to a set of stacked, MOS2, band 2 (0.5-1.0 keV), on-axis source profiles. The *bottom row* refers to the MEDIUM, the *top row* to the ELLBETA PSF. *First panels* from the *left*: stacked images (the same in both rows, as the same test data set was used); *Second panels*: the PSF images. *Third panels*: a  $\chi^2$  image of the residuals between the stacked data and the stacked PSF images, where *magenta* represents  $\chi_r^2 = -20$  and *red* corresponds to  $\chi_r^2 = +20$ . The *colour bar* at the bottom corresponds to this image. *Fourth panels*: image of the function  $R$  (definition in text).  $R$  assumes values close to 0 for random deviations between the data and the model, while it approaches +1 (*white*)/-1 (*black*) for systematic positive/negative deviations. The triangular shape of the in-orbit MOS2 source profile as well the spokes are readily apparent in the MEDIUM mode fit residuals which do not model this level of mirror distortion.

Table 2: Extraction region sizes for the spectra presented in Sect. 5.2 (Fig. 5 and 6). The expression in each cell represents the radius of the circular extraction region for the MEDIUM PSF, the sizes of the minor and major axis of the elliptical region for the ELLBETA PSF

| Instrument | Obs.#0502220201<br>(circular) | Obs.#0502220201<br>(elliptical) | Obs.#0206350101<br>(circular) | Obs.#0206350101<br>(elliptical) |
|------------|-------------------------------|---------------------------------|-------------------------------|---------------------------------|
| MOS1       | 800.0                         | 800.1,800.0                     | 1050.6                        | 1084.1,1050.6                   |
| MOS2       | 800.0                         | 801.1,800.0                     | 1290.0                        | 1330.7,1290.1                   |
| pn         | 500.0                         | 500.2,500.0                     | 1212.3                        | 1270.0,1212.3                   |

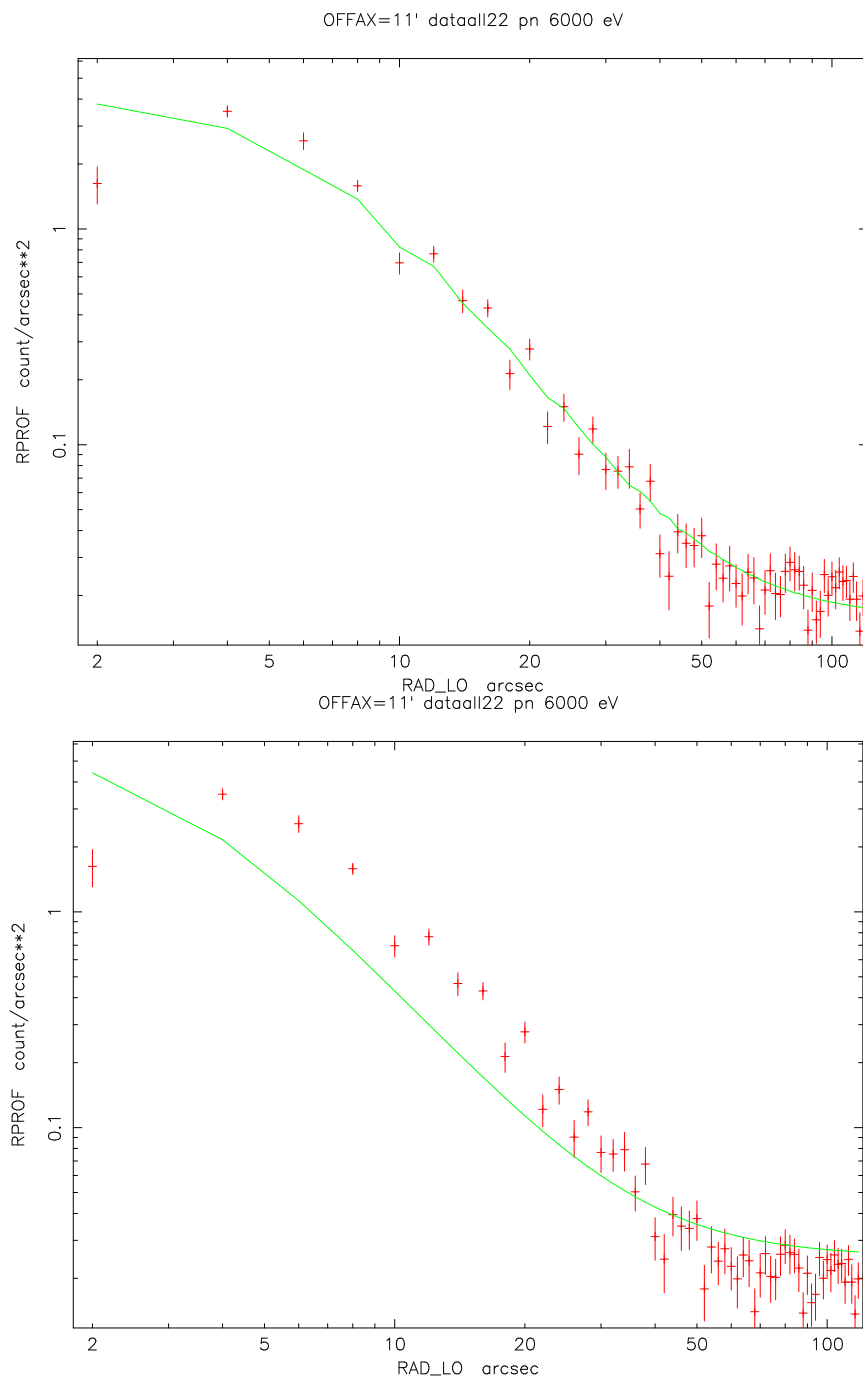
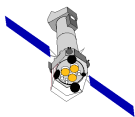


Figure 4: Fits to the 4.5-12 keV radial profile of an EPIC-pn source, 11' off-axis. The data (red points) are fit with a 6 keV ELLBETA model (upper panel, green curve), and a 6 keV EXTENDED PSF model (lower, green curve).



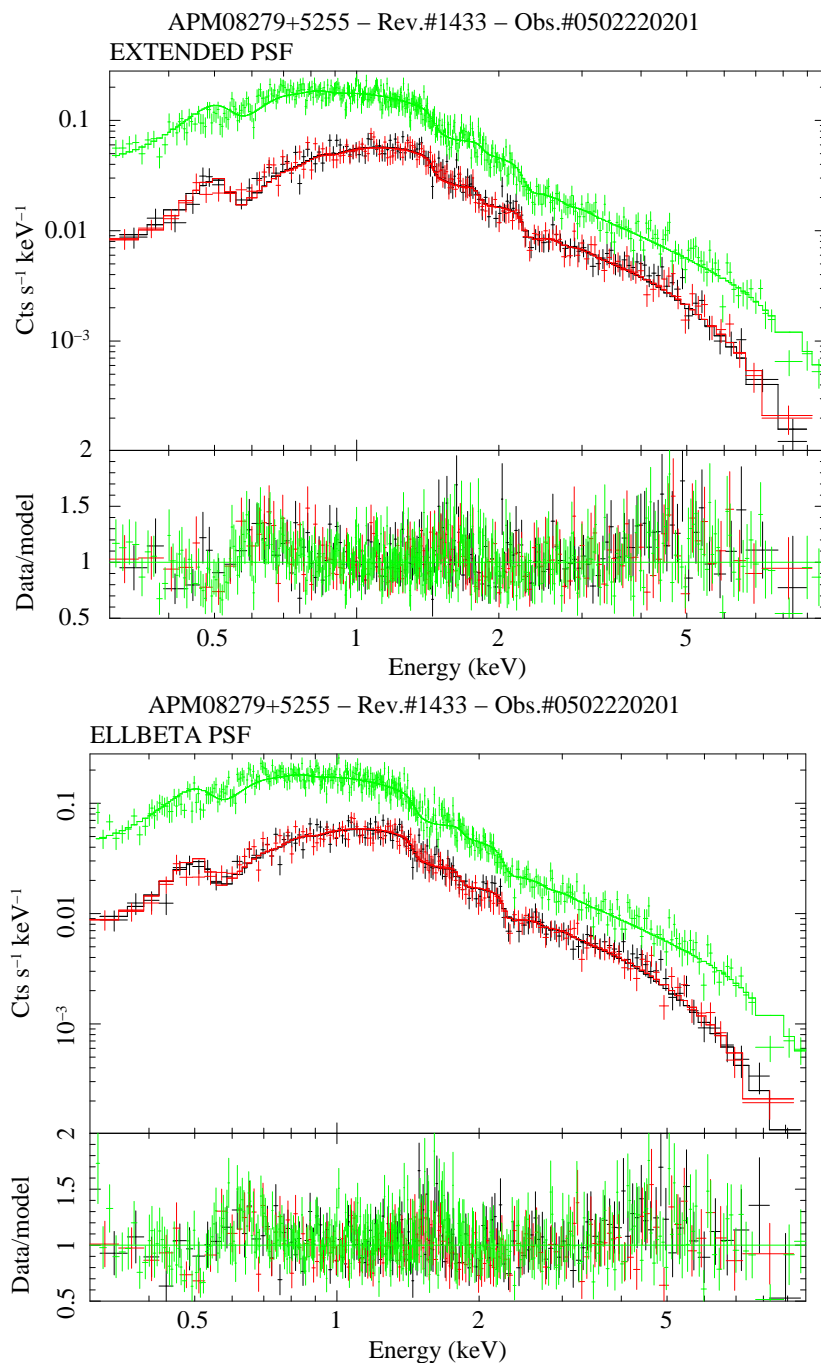
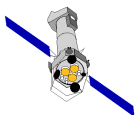


Figure 5: Spectra (*upper panels*) and residuals in units of data/model ratio (*lower panels*) when a photoelectrically absorbed double power-law plus rest-frame neutral iron ( $E_{rest} = 7.11$  keV) photo-absorption edge model is applied to the MOS1 (*black*), MOS2 (*red*) and pn (*green*) spectra of APM08279+5255. The *upper plot* shows spectra extracted with a circular region and the EXTENDED mode PSF; the *lower plot* shows spectra extracted with an elliptical region and the ELLBETA PSF.

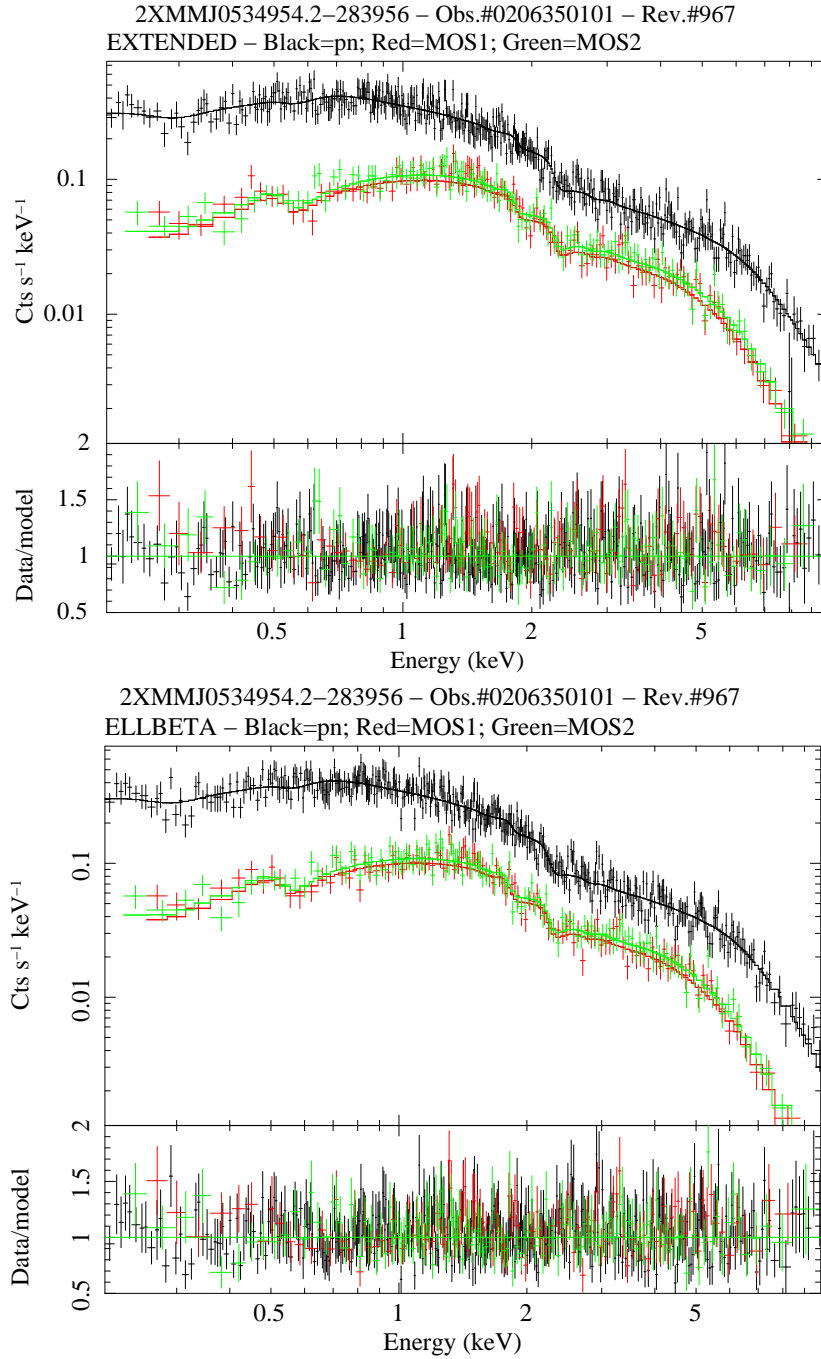
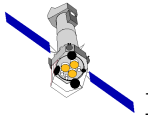
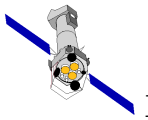


Figure 6: A joint fit with a photoelectrically absorbed broken power-law model to the MOS1/2 and pn observation (Obs.#0206350101) of the non-piled up, 8 arcminute off-axis source, 2XMMJ 053954.2-283956, from Rev.#1801. In the upper panel the EXTENDED PSF is used, while the fit in the lower panel has used the new ELLBETA PSF.



investigated in Fig. 7 for a sample of 24 off-axis sources. The ratio of the MOS1/2 and pn fluxes, calculated using the MEDIUM mode PSF, is plotted against that obtained from the ELLBETA PSF. This ratio is consistent within the errors for most sources and most energy bands but there is a small tendency for the MOS and pn fluxes to agree more closely with the ELLBETA model representation.

This PSF is not validated for use with piled-up sources, where the core of the profile has to be excised by selecting an annular region.

## 6 Expected Updates

The PSF parameters have been calibrated at a discrete, small set of off-axis angles and small set of energies. The CAL software needs to interpolate between these points to generate parameters for a given position and energy. Currently, a linear interpolation is used because the earlier cubic-spline method was shown to have issues at the extremes of the parameter ranges and when parameters vary sharply from one point to the next. Even with the linear method, care needs to be taken to ensure that interpolated values produce a smoothly varying PSF at all positions on the energy/off-axis angle surface. For this reason, adjustments are likely to be needed to some of the parameter values at high energies or high off-axis angles where the quality of the in-orbit data is low.

Further refinements may include, after additional testing:

- calibration refinement of the spoke shape, as well as of the azimuthal filtering, in particular for the pn
- increase of the statistics of the data employed to build the PSF, especially at high energies and large off-axis angles
- exploring a larger parameter space on the new PSF parametrisation impact over detection likelihoods, flux determination, number of spurious sources, measurement of the source extent (or lack thereof) etc.
- proper handling of X-rays not coming from the full annular aperture of the mirrors as you go off-axis *i.e.* the Sagittal-Meridional effect (off-axis and energy-dependent)
- azimuthal dependence of the ELLBETA parameters
- proper handling of dark lanes due to electron deflectors

## Acknowledgments

A careful reading of the manuscript by S.Sembay is gratefully acknowledged.

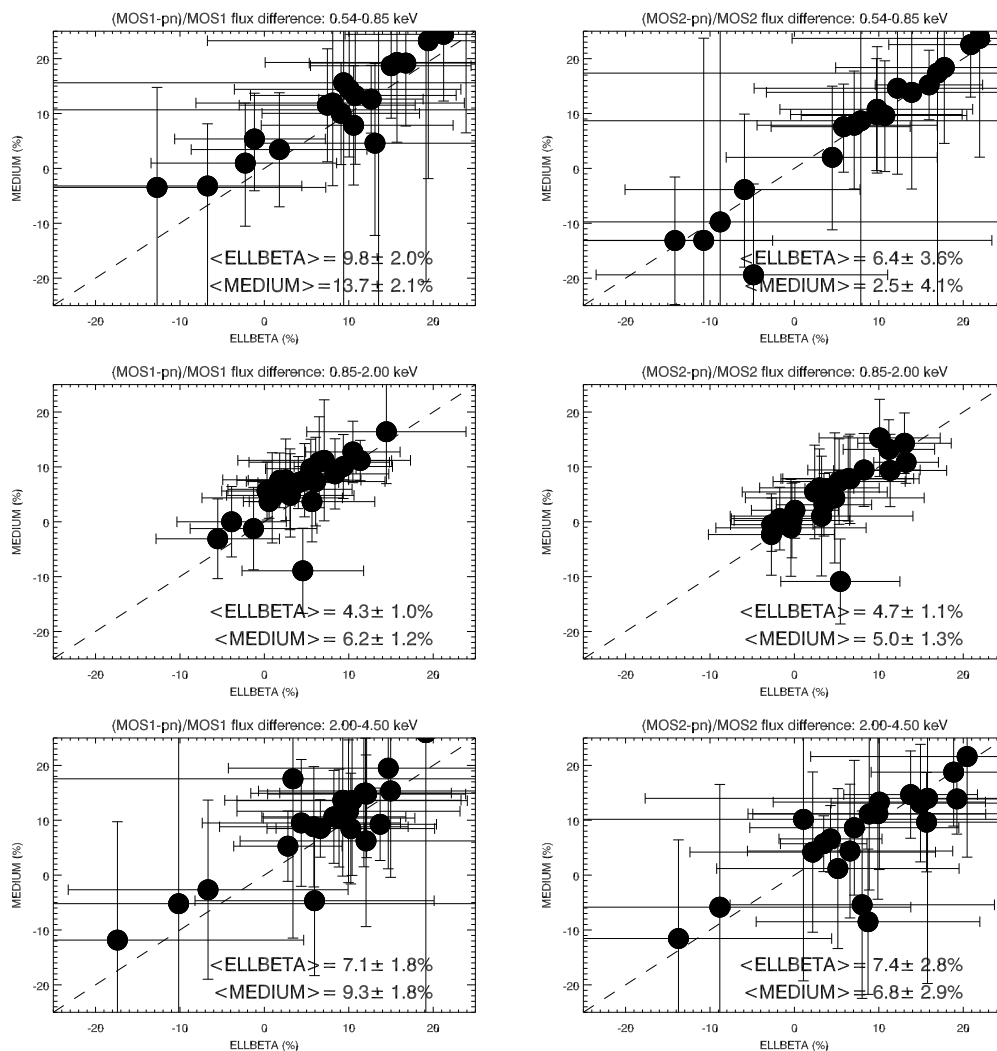
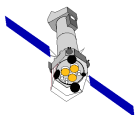
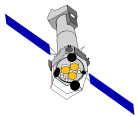


Figure 7: Comparison of the (MOS-pn)/pn flux ratios (in percentage units) in the 0.54-0.85 keV (*upper panels*), 0.85-2 keV (*medium panels*) and 2-4.5 keV (*lower panels*) energy bands between the ELLBETA and the MEDIUM PSF models on the sample of the 24 brightest (in total net counts) off-axis (2 to 12 arcminutes) sources in the 2XMM catalogue (Watson et al. 2009). MOS1: *left*; MOS2: *right*.



## References

Hasinger, G., Schartel, N., Komossa, S. 2002, ApJ, 573, L80.

Watson, M.G., et al., 2009, A&A, 493, 399.